


RESEARCH ARTICLE

Functional connectivity with cortical depth assessed by resting state fMRI of subregions of S1 in squirrel monkeys

Arabinda Mishra^{1,2} | Shantanu Majumdar^{1,2} | Feng Wang^{1,2} | George H. Wilson III^{1,2} | John C. Gore^{1,2} | Li Min Chen^{1,2} 

¹Department of Radiology and Radiological Sciences, Vanderbilt University Medical Center, Nashville, Tennessee

²Vanderbilt University Institute of Imaging Science, Vanderbilt University, Nashville, Tennessee

Correspondence

Li Min Chen, Department of Radiology and Radiological Sciences, Vanderbilt University Institute of Imaging Science, Vanderbilt University Medical Center, 1161 21st Ave. S., AA 1105 MCN, Nashville, TN 37232.
Email: limin.chen@vanderbilt.edu

Funding information

National Institute of Neurological Disorders and Stroke, Grant/Award Number: NS069909, NS078680, NS092961; National Institutes of Health

Abstract

Whereas resting state blood oxygenation-level dependent (BOLD) functional MRI has been widely used to assess functional connectivity between cortical regions, the laminar specificity of such measures is poorly understood. This study aims to determine: (a) whether the resting state functional connectivity (rsFC) between two functionally related cortical regions varies with cortical depth, (b) the relationship between layer-resolved tactile stimulus-evoked activation pattern and interlayer rsFC pattern between two functionally distinct but related somatosensory areas 3b and 1, and (c) the effects of spatial resolution on rsFC measures. We examined the interlayer rsFC between areas 3b and 1 of squirrel monkeys under anesthesia using tactile stimulus-driven and resting state BOLD acquisitions at submillimeter resolution. Consistent with previous observations in the areas 3b and 1, we detected robust stimulus-evoked BOLD activations with foci were confined mainly to the upper layers (centered at 21% of the cortical depth). By carefully placing seeds in upper, middle, and lower layers of areas 3b and 1, we observed strong rsFC between upper and middle layers of these two areas. The layer-resolved activation patterns in areas 3b and 1 agree with their interlayer rsFC patterns, and are consistent with the known anatomical connections between layers. In summary, using BOLD rsFC pattern, we identified an interlayer interareal microcircuit that shows strong intrinsic functional connections between upper and middle layer areas 3b and 1. RsFC can be used as a robust invasive tool to probe interlayer corticocortical microcircuits.

KEYWORDS

BOLD, cortical layer, resting state functional connectivity, somatosensory

1 | INTRODUCTION

The brain is constantly active, even in the absence of any explicit sensory input or behavioral task. Measurements of the correlations in low frequency temporal fluctuations in MRI signals between different areas at rest, termed resting state functional connectivity (rsFC), provide insight into the intrinsic functional architecture that regulate brain functions and possibly into the changes associated with neurological diseases (Biswal, Yetkin, Haughton, & Hyde, 1995; Fox, Corbetta, Snyder, Vincent, & Raichle, 2006; Fox & Raichle, 2007; Fox, Snyder, Vincent, & Raichle, 2007). Execution and maintenance of many brain functions require coordinated activity of brain structures

across different scales of brain networks, ranging from macroscale global networks (in centimeter to tens of centimeter; e.g., default mode network), local mesoscale networks (in hundreds of micrometers to several millimeters; e.g., functionally specific digit modules within the primary somatosensory cortex, S1), and microscale networks (i.e., at cellular level). At the mesoscale level, modules or columns are believed to be the fundamental building blocks of cortical specialization, and these are often composed of functionally similar neurons (Sur, Merzenich, & Kaas, 1980), for a review see (Ichinohe, 2012). Individual digit regions in sub-regions of S1 cortex (i.e., areas 3a, 3b, 1, and 2) are classical examples of such modular structures. Clustered populations of neurons are thought to permit more efficient

information processing and functional segregation. In contrast to the many studies of macroscale whole brain global networks, few reports have focused on the functional architecture and connectivity network at the columnar and laminar mesoscale levels, partially due to spatial resolution limits imposed on human functional MRI (fMRI) studies (Feinberg, Vu, & Beckett, 2017; Scheeringa, Koopmans, van Mourik, Jensen, & Norris, 2016; Yacoub, Harel, & Ugurbil, 2008). By taking advantage of high signal and contrast-to-noise ratios at high field (i.e., 9.4T), we have previously shown that individual digit regions in areas 3a, 3b, and 1/2 of the S1 cortex exhibit strong rsFC in monkeys (Chen et al., 2011; Wang et al., 2013) and the interregional connectivity strength correlated closely with the location and coherence of local field potential signals (Shi et al., 2017; Wilson, Yang, Gore, & Chen, 2016). In the present study, we focused on the modular, single digit regions of functionally related areas within 3b and 1 of S1, and aimed to measure the patterns of rsFC between different laminar layers in between area 3b and area 1 using blood oxygenation-level dependent (BOLD) contrasts.

Information is processed across different cortical layers both within and between different cortical regions (for reviews on cortical microcircuits, see Douglas and Martin (2004); Opris (2013); Thomson and Bannister (2003)). For example, the six horizontal laminae are often grouped into three classes of neurons: supragranular layers (I–III), a granular layer (IV), and two infragranular layers (V and VI). The functions of each layer are distinct. Of the supragranular layers (I–III), layer III receives input from other cortical columns, and cells in layers II and III project to other parts of the cortex. The granular layer of early sensory cortex (IV) receives inputs from the thalamus and sends signals to the other layers of the column (primarily up to layers II and III). Infragranular layers (V and VI) receive input from the supragranular cells of adjacent columns, and send signals mainly to extracortical structures (e.g., thalamus and other subcortical structures). Moreover, different layers are comprised of different proportions of excitatory and inhibitory neurons, and imbalances of excitation and inhibition across cortical layers have been linked to mental disorders. The anatomical connections between layers are well established, so the examination of functional connectivity between layers of functionally related regions may provide valuable insights into local and interareal information flow for specific brain functions, such as the somatosensory functions studied here or visual cortex in humans (Scheeringa et al., 2016).

To date, numerous studies have explored how fMRI responses to stimulation differ with cortical depth (Baek et al., 2016; Bissig & Berkowitz, 2009; Chen, Wang, Gore, & Roe, 2013; Guidi, Huber, Lampe, Gauthier, & Moller, 2016; Harel, Lin, Moeller, Ugurbil, & Yacoub, 2006; Herman, Sanganahalli, Blumenfeld, Rothman, & Hyder, 2013; Koopmans, Barth, & Norris, 2010; Lu et al., 2004; Polimeni, Fischl, Greve, & Wald, 2010; Silva & Koretsky, 2002; Zhao, Wang, Hendrich, Ugurbil, & Kim, 2006). Several previous studies have indicated that stimulus-evoked fMRI activation varies between specific layers (Chen et al., 2013; Goense, Merkle, & Logothetis, 2012; Koopmans et al., 2010; Polimeni et al., 2010; Poplawsky & Kim, 2014). Few studies have compared directly the patterns of layer-resolved BOLD activation and interlayer rsFC between functionally related cortical areas at columnar scale, and effects of voxels on correlation measures of

resting state BOLD signals. A better understanding of interlaminar functional connectivity should provide insights into the mesoscale functional organization of the cerebral cortex and local mechanisms of encoding neuronal information.

In this study, we specifically address three specific questions: (a) how does rsFC between two functionally related regions vary with depth; (b) what are the relationships between tactile stimuli-evoked activations and interlayer rsFC at different cortical depths; and (c) what is the effects of spatial resolution on rsFC measure? We used tactile stimulus-evoked BOLD activations in areas 3b and 1 to identify seed regions for analyzing functional connectivity between layers. The high sensitivity and spatial resolution of fMRI signals at 9.4T permitted comparisons of functional maps at sub-millimeter resolutions ($0.547 \times 0.547 \times 1$ and $0.273 \times 0.273 \times 1$ mm³). We found layer-preferred (or depth-dependent) functional connections between superficial and middle layers of digit regions in areas 3b and 1. The connectivity and activation pattern are in general agreement. The term “layer” used throughout the manuscript is intended to indicate the three main sections (upper, middle, and lower) of the cortex, not the layers based on cortical cytoarchitectonic features.

2 | METHODS

2.1 | Animal preparation

Four adult male squirrel monkeys were included in this study. Each animal was initially sedated with ketamine hydrochloride (10 mg/kg) and atropine (0.05 mg/kg), and then anesthetized with isoflurane (0.5–1.0%) delivered with N₂O:O₂ (70:30) mixture during the entire imaging session. The level of isoflurane was maintained constant (~0.8%) during the fMRI data acquisitions. The animals' heads were physically stabilized in an MR-compatible frame to minimize motion related artifacts while they were artificially ventilated. Vital signals (i.e., heart rate, respiratory pattern, core temperature, ETCO₂, and pulse oximetry) were monitored and maintained at appropriate levels throughout the imaging session. The Institutional Animal Care and Use Committee at Vanderbilt University approved all procedures performed.

2.2 | MRI data acquisition

All MRI scans were performed on a 9.4 MRI/MRS Varian Inova spectrometer (Varian Inc., Palo Alto, CA) using a 3-cm diameter transmit-receive surface coil positioned over the central and lateral sulci, where the targeted S1 and S2 cortices reside. A set of anatomical images (coronal, axial, and oblique) was used to guide the placement of trans-cortical imaging planes through the digit regions in areas 3b and 1 within S1 (Figure 1b,d). To be able to capture digit activations in areas 3b and 1 in the same sagittal slice, we first typically mapped single digit activations on oblique coronal image planes for each animal, and used these activation maps to guide the placement of sagittal images that are perpendicular to the pial surface of the activation foci (Figure 1d). Figure 1 illustrates our image acquisition strategy. The centers of area 3b and area 1 activations to single digit stimulation

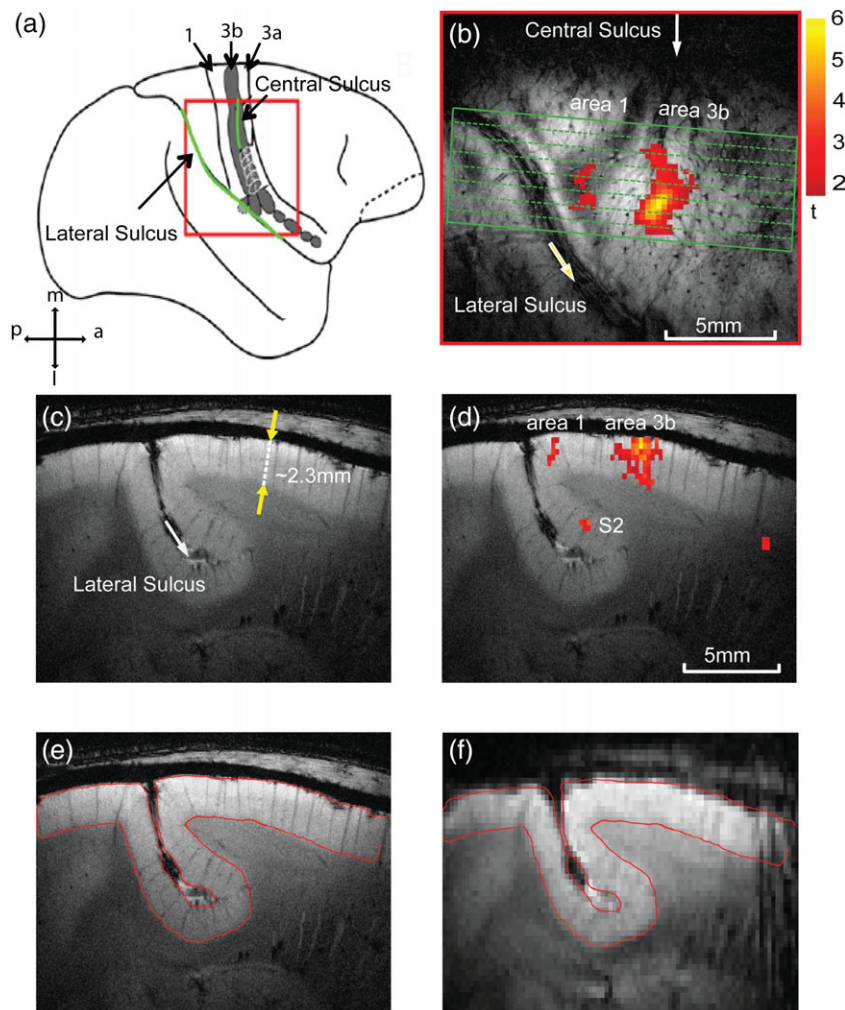


FIGURE 1 Image placements for mapping laminar structure and functions of areas 3b and 1 of primary somatosensory cortex (S1) in squirrel monkeys. (a) Side view of the S1 (areas 3a, 3b, 1) cortex around the central and lateral sulci (green lines) on schematic brain drawing. 1: area 1, 3b: area 3b, 3a: area 3a. Red box: the field of view for oblique MRI image acquisition (shown in b). m: middle, l: lateral, p: posterior, a: anterior. (b) Oblique T_2^* -weighted MRI image shows the imaging field of view over the S1 cortex and an activation focus to D2 tactile stimulation. The green box indicates the location and tissue coverage of the oblique sagittal MRI images. Scale bar: range of t values. (c) T_2^* -weighted structural MRI sagittal image shows the laminar structure of the S1 cortex. The yellow arrows refer to the thickness of the cortex in a direction perpendicular to the cortical surface. (d) Overlaid BOLD activation to D2 tactile stimulation (yellow–red patch) on structural MRI image. (e, f) Manually aligned anatomic (e) and EPI BOLD (f) images. The red outline shows the gray matter boundary derived from anatomic image (e) [Color figure can be viewed at wileyonlinelibrary.com]

were aligned in one slice to minimize the potential influence of slice timing differences. Eight 1-mm thick T_2^* -weighted trans-cortical sagittal structural images were acquired (TR = 200 ms, TE = 16 ms, in-plane resolution of $68 \times 68 \mu\text{m}^2$). Multiple runs (6–12) of resting state and stimulus-driven fMRI data (300 volumes per run) were acquired using a multishot gradient-echo planar imaging sequence for each of two in-plane resolutions: $0.273 \times 0.273 \text{ mm}^2$ (four shots, TR = 3 s) and $0.547 \times 0.547 \text{ mm}^2$ (two shots, TR = 1.5 s).

An innocuous 8 Hz vibrotactile stimulus was delivered with 20 ms pulses on individual distal finger pads separately (typically D2 or D3), by vertical indentation of the skin (0.34 mm displacement) with a plastic probe (2 mm in diameter) mounted on a piezoceramic actuator (Noliac) driven by a Grass Instruments stimulator. Vibrotactile stimuli were presented for seven alternating 30 s off/on blocks to elicit stimulus-driven activations.

2.3 | fMRI data preprocessing

All fMRI data preprocessing was performed in MATLAB 16. FMRI BOLD images from each run underwent slice time correction, followed by 2D motion correction using *spm12*. Six parameters of motion, along with temporal signals extracted from selected white matter voxels containing at least 70% of the cumulative variance (derived using principal components analysis) were considered nuisance parameters and regressed out using a general linear model. Spatial smoothing was not performed. The fMRI signals were then corrected for physiological noise using RETROICOR (Glover, Li, & Ress, 2000). Resting state fMRI signals were bandpass filtered (Chebyshev type 2 IIR filter, cut-off frequencies 0.008 and 0.08 Hz) prior to voxel-wise and pairwise correlation analyses. Stimulus-driven fMRI signals were low-pass filtered with a high frequency cutoff to 0.25 Hz for low-resolution ($0.547 \times 0.547 \times 1 \text{ mm}^3$) data only. No

low-pass filtering was performed on the high-resolution data due to the longer TR (3 s). A temporal signal-to-noise mask (tSNR > 10) was used to eliminate nonbrain voxels for both stimulus-driven activation and resting state connectivity analyses. Occasionally, a manually outlined muscle mask was also used to eliminate muscle voxels in the analysis. To accurately localize different layers on sagittal images, we manually coregistered the high-resolution structural and fMRI (BOLD) images slice by slice in each run. Representative slices of coregistered BOLD and the structural images are shown in Figure 1e,f.

2.4 | Detection of stimulus-evoked activations

To localize the stimulus-driven activation in S1 cortex, we performed voxel-wise analyses of BOLD signal time courses using a generalized linear model (GLM, *spm12*). For each run, activated voxels were defined as those showing stimulus-related signal changes at a statistically significant level of $p < .05$ with family wise error (FWE, *spm12*) correction and clustering of a minimum of two contiguous voxels. The activation maps were displayed as t statistic (t value) maps. The default hemodynamic response function in *spm12* was used to model the stimulus-driven BOLD signal changes.

The time courses of two activated voxels with the highest t values in area 3b were averaged across stimulus epochs ($n = 7$ within each run), runs ($n = 5$), and animals ($n = 3$ for low resolution and $n = 4$ for high resolution data) and presented as percentage signal change. Two time points before the onset of the stimulus were considered as the base line signal amplitude for calculating percentage fMRI signal changes. The depth of each activation focus within the cortex was measured as the distance between the peak activation voxel perpendiculars to the pial surface (gray matter–cerebrospinal fluid boundary). As the orientation of the cortex in reference to the 2-D image space (x, y directions) varies from animal to animal, we measured the shortest distance from the cortical surface in voxel units in both x and y directions. The Euclidean distance in millimeter is then calculated by dividing the distance in the y direction by the cosine of the angle, which varies from 20° to 40° for different animals. The dotted line in Figure 1c, which is in a direction perpendicular to the cortical surface, forms an oblique angle ($\theta \approx 20^\circ$) with the y axis in the image space. All calculations of the depth of functional activation in areas 3b and 1 are calculated in a similar manner. The above parameters were measured separately for two spatial resolutions. We also quantified the spatial and temporal SNR (SNR and tSNR) across layers in area 3b (Figure 4c). Both values were calculated by defining a window (roughly 5 mm in width) comprising seven voxels in the high-resolution data.

2.5 | Defining seeds for interlaminar resting state connectivity analysis

To accurately define the seeds in three different layers, we first measured the cortical thicknesses of areas 3b and 1 and then divided them into three equal sections. Defining the interface between gray matter and CSF around S1 region where the BOLD response occurs is a crucial step in measuring the thickness of cortex of areas 3b and 1. In most of the images, the orthogonal line to the gray matter and CSF interface was not parallel to the y axis (vertical) and usually intersects

with an angle of $\sim 20^\circ$. Under such conditions, we calculated the Euclidian distance (ED) based on the position of the voxels along the orthogonal line, and compensated the ED measure by dividing by the cosine of the angle on a case-by-case basis.

We then defined the regions that showed the strongest responses to tactile stimuli of digits as the seeds regions in areas 3b and 1. At each digit location (e.g., D2 regions in areas 3b and 1), we divided the entire thickness of the cortex (measured as ~ 2.3 mm in depth, Figure 1c) into three equal sections orthogonal to the cortical surface, representing three separate layer sections. To minimize partial volume effects, within each session, typically one voxel in the low-resolution and two to three voxels in the high-resolution image set, which showed strongest responses to stimuli, were selected in each layer from one horizontal voxel line as the seed(s) for interregional correlation analyses (see Figure 5a as an example). In general, activation in area 1 was weaker; hence, fewer voxels were above the threshold than those in area 3b when the same p value threshold was applied. In cases where no strong activated voxels were detected in area 1, activation maps obtained from other imaging sessions from the same animal were used to guide the placement of the area 1 region of interest. The thickness of the cortex in the sagittal slice of high-resolution data includes roughly two times the number of voxels as the low-resolution data, so we selected two to three peak voxels in each layer as the seed. The maximally correlated voxel pairs and corresponding r values were chosen for quantification. Pairwise interregional correlation analyses were performed between all possible combinations of the six seed pairs (three-layer seeds in each of areas 3b and 1).

2.6 | Statistical analysis

We performed analysis of variance (ANOVA) to examine whether the resting state correlations differed significantly between: (a) different layers of areas 3b and 1, and (b) two different spatial resolutions. One-way ANOVA was followed by multiple comparisons to determine the statistical significance of differences between specific pairs of interlayer correlations at a group level. Two-way ANOVA was used to examine the effect of resolutions on the correlations between corresponding pairs of layers defined within area 3b and 1. We also performed the nonparametric Mann–Whitney–Wilcoxon (MWW) test to determine whether the correlation differences are significant.

3 | RESULTS

3.1 | Reproducible stimulus-evoked fMRI activations along cortical depth

Figure 2 illustrates the reproducible BOLD (Figure 2a) activation responses in area 3b to D2 stimulation in two successive fMRI runs for a representative subject. The strongest activation foci were detected in upper layers (see the yellow voxels in slice 2 for BOLD), with relatively weak but spatially similar activations in the two contiguous slices. The positions of activated voxels across multiple runs were spatially well aligned with each other. We calculated the

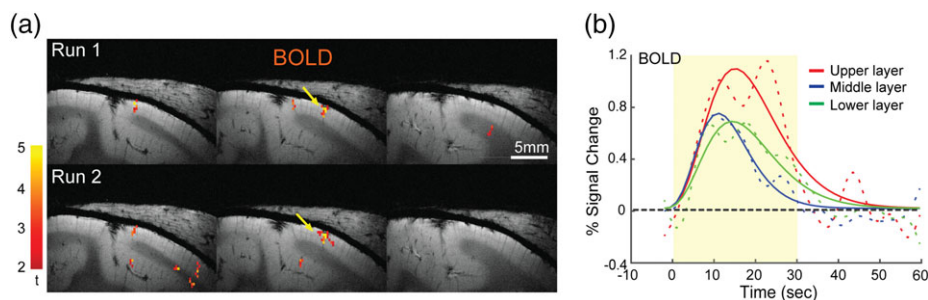


FIGURE 2 Reproducible tactile activation across cortical layers of area 3b. (a) Reproducible and localized BOLD activation maps (in $0.273 \times 0.273 \text{ mm}^2$ in-plane resolution) to D2 stimulation in area 3b across three adjacent slices in two runs acquired in the same session in one representative subject. The yellow arrow indicates the centers (highest t value) of the activation foci. Color scale: range of t values. (b) Mean raw (dotted lines) and single gamma-fitted (solid lines) % BOLD signal changes extracted from three layers. Light yellow shaded box represents the 30 s stimulus on cycle [Color figure can be viewed at wileyonlinelibrary.com]

percentage BOLD signal changes in the peak voxels of area 3b in the low-resolution data during tactile stimulation of individual distal finger pads, and then averaged these signal changes over multiple runs ($n = 6$) within each session and across subjects ($n = 3$). Figure 2b illustrates the overall shape of the time courses of BOLD derived from three layers. Calculation of the percentage signal changes along the direction perpendicular to the pial surface for three layer sections localized the peak response to the upper layer for BOLD (red lines in Figure 2b). The peak percentage signal changes derived from one-gamma fitting (solid lines) of the raw mean signal changes (dotted color lines) were 1.10, 0.75, and 0.69% for BOLD. Figure 3 shows that robust D2 tactile stimulus-evoked BOLD (red–yellow patches in Figure 3a,b) activations were detected in areas 3b and 1 in both high- and low- resolution fMRI data sets (thresholded at $t > 2$, $p < 0.05$, corrected for multiple comparisons) in a representative subject. The strongest BOLD responses (highest t value, yellow voxels in Figure 3a,

b) were located in upper layer. Figure 3c shows the distributions of t values as a function of cortical depth for BOLD signal changes.

We further quantified the depths of BOLD activation foci at the group level (Figure 3d, $n = 4$ animals, 18 runs in total). The mean cortical thickness of area 3b was $2.31 (\pm 0.14)$ mm. Using the pial surface as a reference, the group mean depths of BOLD (Figure 3d) activation centers were 0.5 ± 0.07 mm (low resolution) and 0.49 ± 0.04 , (high resolution), which equal to 21% of the total cortical depth.

3.2 | Layer-specific rsFC between areas 3b and 1

After localizing the single digit regions using stimulus-driven activation maps, we performed a seed-based pairwise resting state connectivity analysis between layers of areas 3b and 1. Figure 4 shows the resting state connectivity maps of the *middle* layer seeds in two separate runs of high-resolution BOLD data. Strong correlations were observed between the area 3b middle-layer seed voxels and the middle-layer

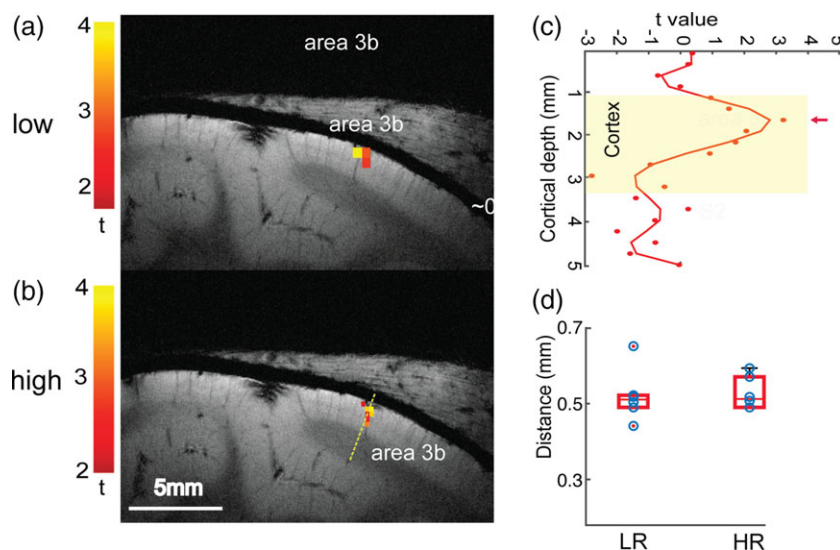


FIGURE 3 Comparison of BOLD tactile activation maps across cortical layers at two spatial resolutions. (a, b) Low- (a) and high-resolution (b) BOLD activation maps in areas 3b and 1 to D2 tactile stimulation in one representative subject. All activation maps were thresholded at $p < .05$ (FWE corrected). Color scales represent t values. (c) 1-D plot of the distribution of t values (color dots) measured (mm) along the yellow dotted line in B, starting from the CSF extending over the white matter through the cortex. High-order polynomial ($n = 8$) fitting was used to illustrate the BOLD peak activation foci. The yellow background shows the width of the cortex. (d) Boxplot shows the distribution of the cortical depth of activation of BOLD signals from the cortical surface for low- (LR) and high-resolution (HR) data. Individual data points are presented using blue circles [Color figure can be viewed at wileyonlinelibrary.com]

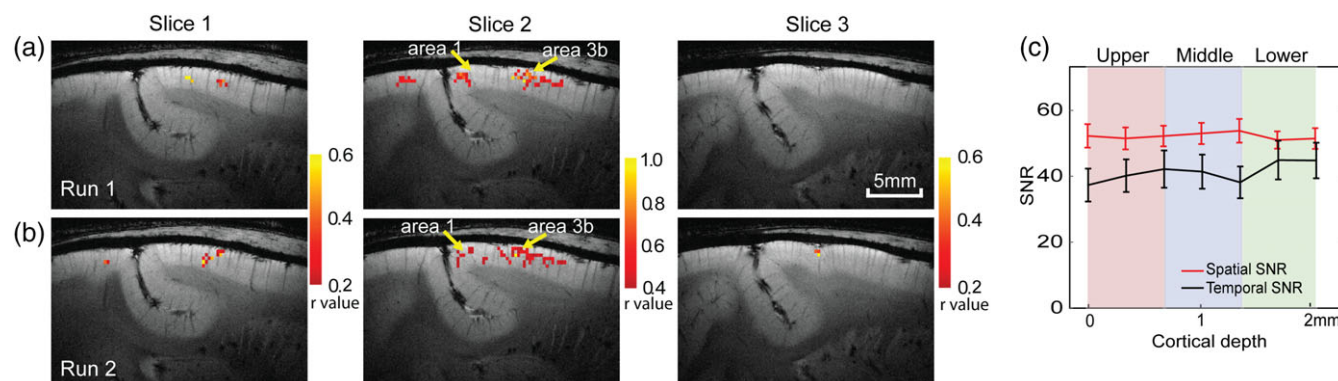


FIGURE 4 The similarity of HR rsFC maps in areas 3b and 1 in one representative subject. Voxel-wise correlation maps of BOLD signals of the ROI seeds in area 3b on three consecutive image slices across two runs (a, b). The single voxel ROI seeds (yellow arrows) in the middle layer were defined by the voxel showing the most robust responses to tactile stimulation. Color bars: range of r values. (c) Plots of mean and SE distribution of spatial (solid lines) and temporal (dotted lines) SNRs of the BOLD (red line) signals along cortical depth in area 3b. Measures were derived from 12 runs ($n = 3$ animals, six runs in each group), respectively [Color figure can be viewed at wileyonlinelibrary.com]

voxels in adjacent slices as well as corresponding layers in area 1 (yellow arrows in Figure 4). The local and interareal (between areas 3b and 1) correlation strengths within the seed slice were stronger than those on adjacent slices. The r threshold on adjacent slices was selected at lower value to show the correlated regions. To evaluate whether or to what extent the interlayer FC differences measured by BOLD signals are related to the signal or noise variations along the cortical depth, we quantified the spatial and temporal signal-noise ratio (SNR and tSNR) in area 3b (Figure 4c). The mean SNR and tSNR plots of the resting state BOLD signals (solid and dotted red lines in Figure 4c) measured across 12 runs ($n = 3$ animals and a total of 12 runs, four runs from each animal) showed a fairly even distribution across three layers, with no systematic trend of variations across the layers.

We further examined the degree to which functional connectivity is layer-specific by selecting seeds in all three layers. Red–yellow voxels in Figure 5a showed the local distribution of BOLD responses to D2 stimulation in areas 3b and 1 (thresholded at $t > 2$) in a representative subject. The voxels with asterisk displayed the strongest responses to stimuli, measured as the highest t values within each layer specified by the white grid, and were chosen as seed voxels for rsFC analysis. For BOLD resting state signals, translation of the area 3b seed from the upper to lower layers (Figure 5b) resulted in a similar translation of highly correlated voxels in corresponding area 1.

3.3 | Group comparison of interlayer functional connectivity differences between areas 3b and 1 in high versus low resolutions

We calculated the average group-level layer-specific pair-wise functional connectivity strength values for BOLD signals at two resolutions ($0.547 \times 0.547 \times 1 \text{ mm}^3$ vs. $0.273 \times 0.273 \times 1 \text{ mm}^3$, Figure 6). The overall interlayer correlation strengths (r values) of BOLD resting state signals between different layers of areas 3b and 1 are shown in the 2D matrix plots in Figure 6 (low resolution in a; high resolution in b). These matrices clearly show stronger functional connectivity (see the orange–red elements) between the upper and middle layers of

areas 3b and 1 for the BOLD signals (left two columns) for both resolutions. The layer pairs showing significant correlation (rsFC) differences were connected with color dotted lines on the matrix.

We performed a one-way ANOVA followed by an MWW nonparametric test to evaluate the statistical significance of the differences in the correlations between different layer pairs. Consistent with the 2D matrix plots (dotted light blue lines in Figure 6a,b), we found that the strengths of upper-to-upper connectivity between areas 3b and 1 were significantly stronger ($p < .05$, MWW test) than that of upper-to-low connectivity for the BOLD signals for both resolutions (left column groups in Figure 6c,d). For low-resolution data, upper-to-middle connectivity was also stronger than that of upper-to-lower

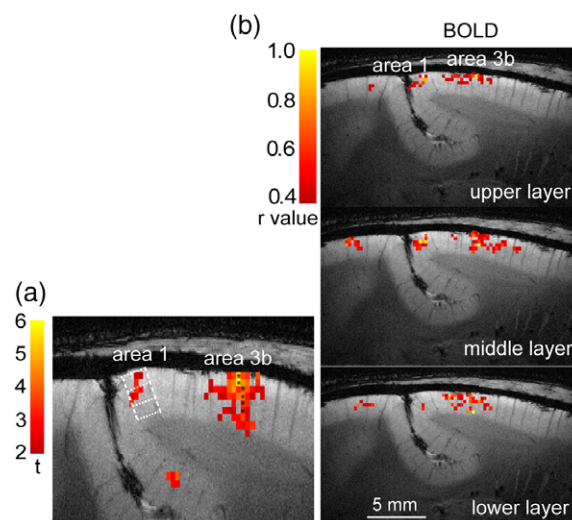


FIGURE 5 Layer-specific BOLD rsFC maps between areas 3b and 1 in one representative subject. (a) Tactile stimulus-evoked BOLD activation map (thresholded at $t > 2.0$, HR data) shows the selection of seed voxels (black stars) in each layer of area 3b. Dotted white lines indicate the estimated interlaminar borders. (b) Voxel-wise BOLD correlation maps of seeds in upper, middle, and lower layers of area 3b. Correlation maps are thresholded at $r > .4$. Color bars indicate the range of r values [Color figure can be viewed at wileyonlinelibrary.com]

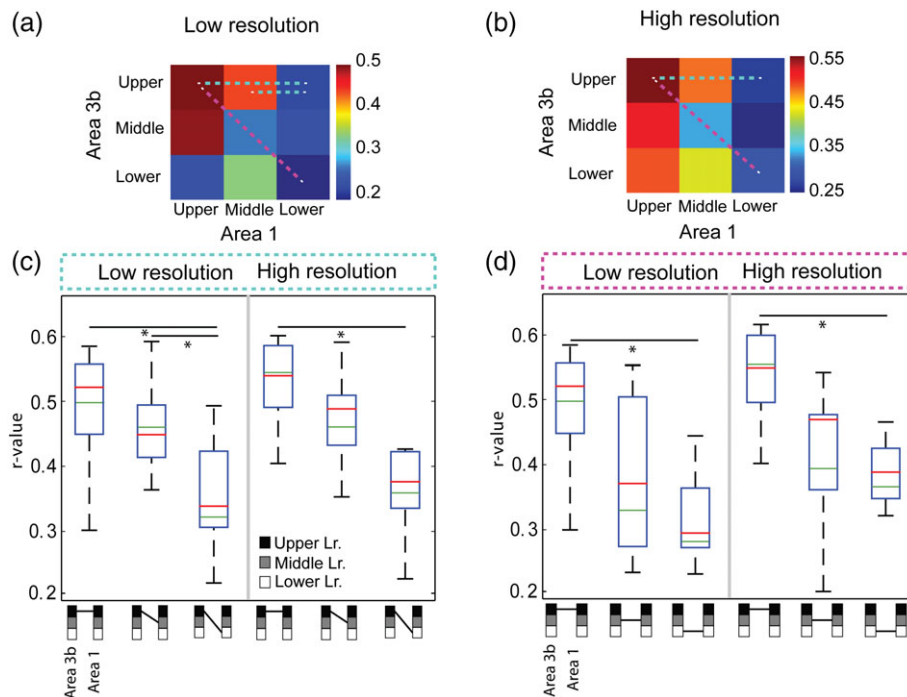


FIGURE 6 Group quantification of interlaminar rsFC of BOLD signals between areas 3b and 1 at low and high resolutions. (a, b) 2D matrix plots of pairwise interlayer mean correlations (r values) of BOLD signals between upper, middle, and lower layers of areas 3b and 1 at low (a) and high (b) resolutions. Dotted color lines link the layer pairs showing statistically significant correlation differences. (c, d) Boxplots of the distributions of rsFC (r values) between specific layer pairs of areas 3b and 1 for low- (c) and high-resolution (d) rsfMRI data. Green line: mean. Red line: median values across the runs and animals ($n = 4$). Symbols below the x axis represent the specific pair of layers examined (linked by short black lines; black: upper, gray: middle, white: lower). These values were included in the statistical test. $*p < .05$, (MWW, Mann Whitney Wilcoxon test, FWE multiple comparison corrected). Symbols below the box plots represent the different pair of layers. Layers are linked by short black lines; black square: upper layer, gray square: middle layer, white square: lower layer [Color figure can be viewed at wileyonlinelibrary.com]

(Figure 6a). Upper-to-upper connectivity between areas 3b and 1 was also stronger than that between middle-to-middle layers for both resolutions ($p < .05$, MWW test; Figure 6c,d. dotted magenta lines in Figure 6a,b). These results confirm that interlayer connectivity was higher between more superficial layers (i.e., upper and middle). All the statistical tests were multiple comparison corrected. As a control, Figure 7 illustrates the distributions of t values and percentage signal changes for both BOLD signals with cortical depth, supporting the fact that at high MRI field stimulus-evoked BOLD activations are focal and robust.

In summary, we have detected peripheral stimuli-evoked BOLD signal changes in predominantly superficial and middle layers in areas 3b and 1, findings that are consistent with previous reports. One step further, we found that resting state BOLD signals identified strong interlayer rsFC patterns between upper and middle layers of two functionally distinct but related somatosensory areas 3b and 1. Increased spatial resolution did not alter the interareal and interlayer intrinsic rsFC patterns. This type of microcircuit between layers of different functional areas differs from the commonly reported microcircuit among upper (supragranular), middle (granular), and lower (infragranular) layers within one single cortical region, and are engaged differently in the processing and integration of the tactile inputs. Figure 8b summarizes the main findings of the present study and Figure 8a presents a simplified interlayer interareal microcircuit model that illustrates the anatomical connections between layers of areas 3b

and 1. The microcircuit identified by rsFC (Figure 8b) in general agrees with that indicated by anatomical connections (Figure 8a). Area 1 is considered as a high-order area to area 3b and receives predominantly afferent input from area 3b. The predominant forward afferent

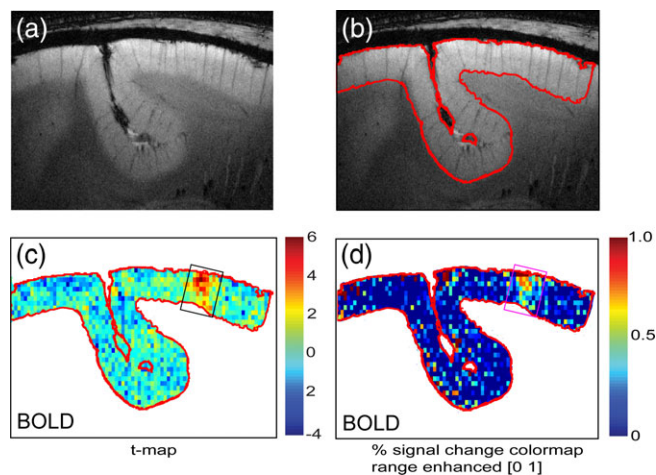


FIGURE 7 Comparison of spatial distribution of t values and percentage signal changes for BOLD in area 3b. (a, b) T_2^* -weighted high resolution structural image (a) with cortex boundary outline (b) from one representative subject. (c, d) t value and percentage signal change maps for BOLD signals. Box outlines indicate the area 3b digit location. Color scale bars: ranges of t value and percentage signal changes [Color figure can be viewed at wileyonlinelibrary.com]

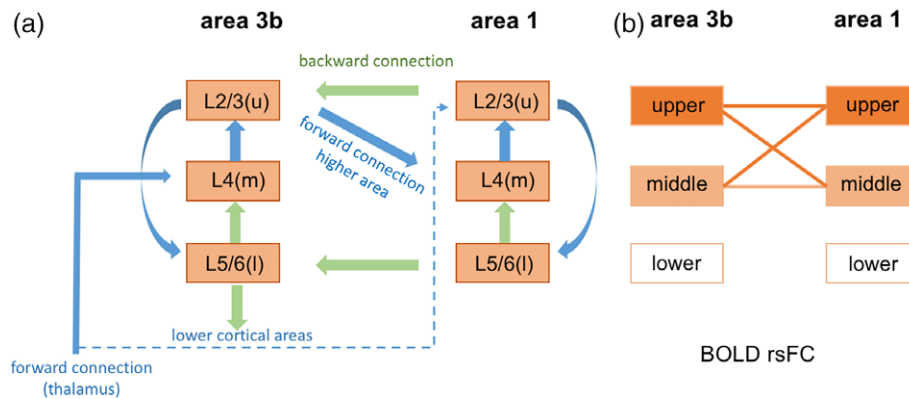


FIGURE 8 Schematic summary of the interlayer microcircuits between areas 3b and 1 and the main findings of the study. (a) The simplified microcircuit of layers within area 3b and between areas 3b and 1 (modified from Bastos et al. (2012)). (b) rsFC pattern between layers of areas 3b and 1. Color lines indicate strong rsFC [Color figure can be viewed at wileyonlinelibrary.com]

connection to area 3b middle layer (IV) comes from the thalamus. Area 1, however, receives its predominant afferent connections from upper layers of area 3b (blue arrow lines in Figure 8a). There are feedback connections from area 1 to upper and lower layers of area 3b (green arrow lines in Figure 8a). In summary, all three layers between areas 3b and 1 are interconnected anatomically. The diagram is modified based on the published anatomical data from this species (Ashaber et al., 2014; Cerkevich & Kaas, 2018).

4 | DISCUSSION

The overall goal of the present study is to determine whether resting state BOLD fMRI signals can be used to identify intrinsic functional circuits between layers of two functionally distinct but related cortical regions: somatosensory area 3b–area 1. These two early somatosensory areas play central roles in tactile detection and discrimination and form extensive corticocortical anatomic connections in the primate brain. While the majority of layer-resolved fMRI studies focused on examining interlayer activity to external stimuli or correlation at rest, this study focused on inter-areal circuits in layer-resolved details.

4.1 | The agreement between BOLD activation maps and interlayer interareal functional connectivity pattern between areas 3b and 1

To date, a number of studies have explored the nature of laminar differentiation and its rsFC within a single cortical region (Chan et al., 2014; Goense et al., 2012; Guidi, Huber, & Lampe, 2016; Huber et al., 2016; Hyde & Li, 2014; Polimeni et al., 2010; Polimeni, Mianciardi, Keli, & Wald, 2015; Shih et al., 2013; Wang, Robinson, & Deshpande, 2016), but only a very few have examined the characteristics of interlayer functional connectivity between two functionally related cortical areas (Baek et al., 2016; Matsui et al., 2011). In this study, we tested the hypothesis that cortical layers that share similar functions exhibit strongly synchronized BOLD fMRI signal fluctuations at rest (Shi et al., 2017; Wang et al., 2013; Wilson et al., 2016). This hypothesis is derived from our previous observations that cortical columns (such as

single digit regions in areas 3b and 1) that are engaged in the same function (such as processing the same tactile inputs from the digits) exhibit strong functional connectivity at rest. There are tight associations between the patterns of functional responses and interareal rsFC at columnar level (Chen et al., 2011; Wang et al., 2013; Wilson et al., 2016). The functional connectivity pattern also generally agrees with underlying anatomical connection pattern (Wang et al., 2013). Here, we focused our investigation first on the relationships of stimulus-evoked activation pattern, interareal rsFC pattern, and anatomical connections in layer-resolved details. We found that upper and middle layers that responded strongly to tactile stimuli also showed strong upper-to-upper (and middle-to-middle) rsFC for BOLD signals between areas 3b and 1. This observation of tight association between stimulus responsiveness and intrinsic rsFC at different cortical depths between two cortical regions supports our hypothesis. The observation of upper and middle layers dominated BOLD activation in either area 3b or area 1 is consistent with a number of activation studies in early sensory cortices (Goense et al., 2012; Kim & Kim, 2010; Zhao et al., 2006), supporting the technical validity of our approach.

4.2 | The use of resting state fMRI signal in probing interlayer microcircuits between cortical areas

Cortical columns are the basic units for information processing in neocortex. A widely accepted canonical microcircuit model characterizes the processes of information flowing through local, feed forward and feed backward connections between layers within one single cortical area (see left column of Figure 8a for a simplified illustration; Bastos et al., 2012). In our experimental model of area 3b, external tactile information reaches area 3b middle layer (IV) via thalamic afferents, and is then relayed through local interlayer connections within each column. Output signals are sent via superficial (II and III) or deeper (V and VI) layers to higher order area 1 for further information integration and extraction (Felleman & Van Essen, 1991). Almost at the same time (with a very short delay), other higher order areas including areas 1 and S2 can modulate the information processing within area 3b via feedback connections (Figure 8). These corticocortical connections are essential in shape the information integration and abnormalities

are linked to many brain disorders. Currently, there is no established noninvasive method that permits probing of these important cortico-cortical microcircuits in laminar details. Thus, the ability to noninvasively visualize and study their functions connections directly could have a major impact on our understanding of brain function. To date, numerous studies have characterized cortical fMRI response profiles across cortical layers within one single cortical region in humans and animals (Koopmans et al., 2010; Olman et al., 2012; Polimeni et al., 2010; Scheeringa et al., 2016). Here, we demonstrated that rsFC can also be used to probe layer-dependent corticocortical microcircuits. The similarity between the rsFC pattern and underlying anatomical connectivity pattern (Figure 8) indicates the robustness of rsFC in probing these fine-scale functional microcircuits.

4.3 | Possible contributors to the distinct layer-dependent interareal rsFC patterns revealed by resting state BOLD signals

Emerging evidence indicates that depth dependent differences in baseline vascular structure and physiology, neural activity, and/or neurovascular coupling mechanisms can influence the magnitudes of stimulus-evoked activations at different cortical depths (Goense, Bohraus, & Logothetis, 2016; Patel, Kennerley, Boorman, Jones, & Berwick, 2015; Polimeni et al., 2010). For example, several layer-resolved fMRI studies focused on stimulus-evoked or task-associated fMRI responses within a single cortical region found that fMRI signals (BOLD, cerebral blood volume [CBV], and cerebral blood flow [CBF]) responded differently to the same stimulus across layers of visual and somatosensory cortices (Bandettini, 2012; Goense et al., 2012; Goense & Logothetis, 2006; Huber et al., 2015; Huber, Uludag, & Moller, 2017; Maier, Adams, Aura, & Leopold, 2010; Silva & Koretsky, 2002; Tian et al., 2010). Stimulus-evoked BOLD signal changes generally are biased toward upper and middle layers (Poplawsky & Kim, 2014). In our study, the BOLD signal appeared to be weaker than CBV in detecting correlated activity in lower cortical layers (Shih et al., 2013). However, to date, few studies have examined how these vascular factors may contribute and influence the correlation strength between resting state BOLD signals extracted from different layers from two different cortical areas (Huber et al., 2016; Polimeni et al., 2010), (Baek et al., 2016; Tak, Polimeni, Wang, Yan, & Chen, 2015; Tak, Wang, Polimeni, Yan, & Chen, 2014). While in the current study, we did not directly address these questions by comparing rsFC patterns derived from different fMRI signals (e.g., BOLD vs. CBV or CBF), at least we are confident that the interlayer connectivity pattern between areas 3b and 1 are not the byproducts of BOLD signal variation across cortical layers (Goense et al., 2012; Huber et al., 2015; Polimeni et al., 2016; Poplawsky & Kim, 2014). Figure 4c shows that the SNR and tSNR are fairly comparable across layers. Importantly, the areas 3b and 1 of the squirrel monkeys closely located (2–3 mm apart) on a flat cortex and share a very similar blood vessel density, and physiological noise.

Nevertheless, using the known interlayer anatomical microcircuits as a reference (Figure 8a), one would notice that the connections between lower layers of areas 3b and 1 were not detected by resting state BOLD signals (Figure 8b). The failed detection could be an

indication of the upper and middle layer bias of BOLD signal that demonstrated in the stimulus condition, or a relatively weak correlation between lower layers. Future studies that permit direct comparisons between different fMRI signals and between fMRI and electrophysiological signals will provide more conclusive clues about the underlying mechanisms and the influence of vascular features.

A final note is that anesthesia is known to reduce the measured strengths of functional connectivity in an area-dependent manner (Bonhomme et al., 2011; Grandjean, Schroeter, Batata, & Rudin, 2014; Jonckers et al., 2014; Wu et al., 2016). However, to date, there is no evidence suggesting that anesthesia alters synchronization of resting state signals between layers in two functionally highly related cortical areas. In contrast, our own studies found that rsFC patterns did not change as a function of anesthesia level, indicating that the core intrinsic patterns are preserved under the light anesthesia level we used in our studies (Wu, Yang, & Chen, 2017). Increases in anesthesia depth only reduced the overall rsFC strength with no noticeable area bias (Wu et al., 2016).

ACKNOWLEDGMENTS

This work was supported by National Institutes of Health grants R01 NS069909 (to LMC), R01 NS078680 (to JCG), and R01 NS092961 (to J.C.G./L.M.C.). The authors would like to thank Fuxue Xin and Chaoui Tang for their help in acquiring the MRI data and animal care.

ORCID

Li Min Chen  <https://orcid.org/0000-0001-9662-1925>

REFERENCES

- Ashaber, M., Palfi, E., Friedman, R. M., Palmer, C., Jakli, B., Chen, L. M., ... Negyessy, L. (2014). Connectivity of somatosensory cortical area 1 forms an anatomical substrate for the emergence of multifinger receptive fields and complex feature selectivity in the squirrel monkey (*Saimiri sciureus*). *The Journal of Comparative Neurology*, *522*, 1769–1785.
- Baek, K., Shim, W. H., Jeong, J., Radhakrishnan, H., Rosen, B. R., Boas, D., ... Kim, Y. R. (2016). Layer-specific interhemispheric functional connectivity in the somatosensory cortex of rats: Resting state electrophysiology and fMRI studies. *Brain Structure & Function*, *221*, 2801–2815.
- Bandettini, P. A. (2012). The BOLD plot thickens: Sign- and layer-dependent hemodynamic changes with activation. *Neuron*, *76*, 468–469.
- Bastos, A. M., Usrey, W. M., Adams, R. A., Mangun, G. R., Fries, P., & Friston, K. J. (2012). Canonical microcircuits for predictive coding. *Neuron*, *76*, 695–711.
- Bissig, D., & Berkowitz, B. A. (2009). Manganese-enhanced MRI of layer-specific activity in the visual cortex from awake and free-moving rats. *NeuroImage*, *44*, 627–635.
- Biswal, B., Yetkin, F. Z., Houghton, V. M., & Hyde, J. S. (1995). Functional connectivity in the motor cortex of resting human brain using echo-planar MRI. *Magnetic Resonance in Medicine*, *34*, 537–541.
- Bonhomme, V., Boveroux, P., Hans, P., Brichant, J. F., Vanhaudenhuyse, A., Boly, M., & Laureys, S. (2011). Influence of anesthesia on cerebral blood flow, cerebral metabolic rate, and brain functional connectivity. *Current Opinion in Anaesthesiology*, *24*, 474–479.
- Cerkevich, C. M., & Kaas, J. H. (2018). Corticocortical projections to area 1 in squirrel monkeys (*Saimiri sciureus*). *The European Journal of Neuroscience*. <https://doi.org/10.1111/ejn.13884>. [Epub ahead of print]

- Chan, R.W., Fan, S.J., Gao, P.P., Zhou, I.Y., Tsang, A., Wu, E.X. (2014). Lamina-specific profile of intracortical resting-state functional connectivity. In; 2014. p 6590 (ISMRM 2014, May 10-16 Milan, Italy).
- Chen, G., Wang, F., Gore, J. C., & Roe, A. W. (2013). Layer-specific BOLD activation in awake monkey V1 revealed by ultra-high spatial resolution functional magnetic resonance imaging. *NeuroImage*, *64*, 147-155.
- Chen, L., Mishra, A., Newton, A. T., Morgan, V. L., Stringer, E. A., Rogers, B. P., & Gore, J. C. (2011). Fine-scale functional connectivity in somatosensory cortex revealed by high-resolution fMRI. *Magnetic Resonance Imaging*, *29*, 1330-1337.
- Douglas, R. J., & Martin, K. A. (2004). Neuronal circuits of the neocortex. *Annual Review of Neuroscience*, *27*, 419-451.
- Feinberg, D. A., Vu, A. T., & Beckett, A. (2017). Pushing the limits of ultra-high resolution human brain imaging with SMS-EPI demonstrated for columnar level fMRI. *NeuroImage*, *164*, 155-163.
- Felleman, D. J., & Van Essen, D. C. (1991). Distributed hierarchical processing in the primate cerebral cortex. *Cerebral Cortex*, *1*, 1-47.
- Fox, M. D., Corbetta, M., Snyder, A. Z., Vincent, J. L., & Raichle, M. E. (2006). Spontaneous neuronal activity distinguishes human dorsal and ventral attention systems. *Proceedings of the National Academy of Sciences of the United States of America*, *103*, 10046-10051.
- Fox, M. D., & Raichle, M. E. (2007). Spontaneous fluctuations in brain activity observed with functional magnetic resonance imaging. *Nature Reviews Neuroscience*, *8*, 700-711.
- Fox, M. D., Snyder, A. Z., Vincent, J. L., & Raichle, M. E. (2007). Intrinsic fluctuations within cortical systems account for intertrial variability in human behavior. *Neuron*, *56*, 171-184.
- Glover, G. H., Li, T. Q., & Ress, D. (2000). Image-based method for retrospective correction of physiological motion effects in fMRI: RETROICOR. *Magnetic Resonance in Medicine*, *44*, 162-167.
- Goense, J., Bohraus, Y., & Logothetis, N. K. (2016). fMRI at high spatial resolution: Implications for BOLD-models. *Frontiers in Computational Neuroscience*, *10*, 66.
- Goense, J., Merkle, H., & Logothetis, N. K. (2012). High-resolution fMRI reveals laminar differences in neurovascular coupling between positive and negative BOLD responses. *Neuron*, *76*, 629-639.
- Goense, J. B., & Logothetis, N. K. (2006). Laminar specificity in monkey V1 using high-resolution SE-fMRI. *Magnetic Resonance Imaging*, *24*, 381-392.
- Grandjean, J., Schroeter, A., Batata, I., & Rudin, M. (2014). Optimization of anesthesia protocol for resting-state fMRI in mice based on differential effects of anesthetics on functional connectivity patterns. *NeuroImage*, *102*(Pt 2), 838-847.
- Guidi, M., Huber, L., Lampe, L. Cortical Laminar Resting-State Fluctuations Scale with Hypercapnic Response. In; 2016. p 769.
- Guidi, M., Huber, L., Lampe, L., Gauthier, C. J., & Moller, H. E. (2016). Lamina-dependent calibrated BOLD response in human primary motor cortex. *NeuroImage*, *141*, 250-261.
- Harel, N., Lin, J., Moeller, S., Ugurbil, K., & Yacoub, E. (2006). Combined imaging-histological study of cortical laminar specificity of fMRI signals. *NeuroImage*, *29*, 879-887.
- Herman, P., Sanganahalli, B. G., Blumenfeld, H., Rothman, D. L., & Hyder, F. (2013). Quantitative basis for neuroimaging of cortical laminae with calibrated functional MRI. *Proceedings of the National Academy of Sciences of the United States of America*, *110*, 15115-15120.
- Huber, L., Goense, J., Kennerley, A. J., Trampel, R., Guidi, M., Reimer, E., ... Moller, H. E. (2015). Cortical lamina-dependent blood volume changes in human brain at 7 T. *NeuroImage*, *107*, 23-33.
- Huber, L., Handwerker, D. A., Gonzalez-Castillo, J., Jangraw, D., Guidi, M., Ivanov, D., & Bandettini, P. A. (2016). Effective connectivity measured with layer-dependent resting-state blood volume fMRI in humans. *Proceedings of the International Society of Magnetic Resonance in Medicine (ISMRM 2016, May 07-13, Singapore)*, 948.
- Huber, L., Uludag, K., & Moller, H. E. (2017). Non-BOLD contrast for laminar fMRI in humans: CBF, CBV, and CMRO2. *NeuroImage*, pii: S1053-8119(17)30609-2 [Epub ahead of print].
- Hyde, J. S., & Li, R. (2014). Functional connectivity in rat brain at 200 μ m resolution. *Brain Connectivity*, *4*, 470-480.
- Ichinohe, N. (2012). Small-scale module of the rat granular retrosplenial cortex: An example of the minicolumn-like structure of the cerebral cortex. *Frontiers in Neuroanatomy*, *5*, 69.
- Jonckers, E., Delgado y Palacios, R., Shah, D., Guglielmetti, C., Verhoye, M., & Van der Linden, A. (2014). Different anesthesia regimes modulate the functional connectivity outcome in mice. *Magnetic Resonance in Medicine*, *72*, 1103-1112.
- Kim, T., & Kim, S. G. (2010). Cortical layer-dependent arterial blood volume changes: Improved spatial specificity relative to BOLD fMRI. *NeuroImage*, *49*, 1340-1349.
- Koopmans, P. J., Barth, M., & Norris, D. G. (2010). Layer-specific BOLD activation in human V1. *Human Brain Mapping*, *31*, 1297-1304.
- Lu, H., Patel, S., Luo, F., Li, S. J., Hillard, C. J., Ward, B. D., & Hyde, J. S. (2004). Spatial correlations of laminar BOLD and CBV responses to rat whisker stimulation with neuronal activity localized by Fos expression. *Magnetic Resonance in Medicine*, *52*, 1060-1068.
- Maier, A., Adams, G. K., Aura, C., & Leopold, D. A. (2010). Distinct superficial and deep laminar domains of activity in the visual cortex during rest and stimulation. *Frontiers in Systems Neuroscience*, *4*:31, 1-11.
- Matsui, T., Tamura, K., Koyano, K. W., Takeuchi, D., Adachi, Y., Osada, T., & Miyashita, Y. (2011). Direct comparison of spontaneous functional connectivity and effective connectivity measured by intracortical microstimulation: An fMRI study in macaque monkeys. *Cerebral Cortex*, *21*, 2348-2356.
- Olman, C. A., Harel, N., Feinberg, D. A., He, S., Zhang, P., Ugurbil, K., & Yacoub, E. (2012). Layer-specific fMRI reflects different neuronal computations at different depths in human V1. *PLoS One*, *7*, e32536.
- Opris, I. (2013). Inter-laminar microcircuits across neocortex: Repair and augmentation. *Frontiers in Systems Neuroscience*, *7*, 80.
- Patel, P., Kennerley, A.J., Boorman, L., Jones, M., Berwick, J. Does vasomotion alter functional connectivity? A multi-modal study using Optical Imaging Spectroscopy and BOLD fMRI. In; 2015. p 49.
- Polimeni, J. R., Bhat, H., Witzel, T., Benner, T., Feiweier, T., Inati, S. J., ... Wald, L. L. (2016). Reducing sensitivity losses due to respiration and motion in accelerated echo planar imaging by reordering the autocalibration data acquisition. *Magnetic Resonance in Medicine*, *75*, 665-679.
- Polimeni, J. R., Fischl, B., Greve, D. N., & Wald, L. L. (2010). Laminar analysis of 7T BOLD using an imposed spatial activation pattern in human V1. *NeuroImage*, *52*, 1334-1346.
- Polimeni, J.R., Mianciardi, M., Keli, B., Wald, L.L. Cortical depth dependence of physiological fluctuations and whole-brain resting-state functional connectivity at 7T. In; 2015. p 592.
- Poplawsky, A. J., & Kim, S. G. (2014). Layer-dependent BOLD and CBV-weighted fMRI responses in the rat olfactory bulb. *NeuroImage*, *91*, 237-251.
- Scheeringa, R., Koopmans, P. J., van Mourik, T., Jensen, O., & Norris, D. G. (2016). The relationship between oscillatory EEG activity and the laminar-specific BOLD signal. *Proceedings of the National Academy of Sciences of the United States of America*, *113*, 6761-6766.
- Shi, Z., Wu, R., Yang, P. F., Wang, F., Wu, T. L., Mishra, A., ... Gore, J. C. (2017). High spatial correspondence at a columnar level between activation and resting state fMRI signals and local field potentials. *Proceedings of the National Academy of Sciences of the United States of America*, *114*, 5253-5258.
- Shih, Y. Y., Chen, Y. Y., Lai, H. Y., Kao, Y. C., Shyu, B. C., & Duong, T. Q. (2013). Ultra high-resolution fMRI and electrophysiology of the rat primary somatosensory cortex. *NeuroImage*, *73*, 113-120.
- Silva, A. C., & Koretsky, A. P. (2002). Laminar specificity of functional MRI onset times during somatosensory stimulation in rat. *Proceedings of the National Academy of Sciences of the United States of America*, *99*, 15182-15187.
- Sur, M., Merzenich, M. M., & Kaas, J. H. (1980). Magnification, receptive-field area, and "hypercolumn" size in areas 3b and 1 of somatosensory cortex in owl monkeys. *Journal of Neurophysiology*, *44*, 295-311.
- Tak, S., Polimeni, J. R., Wang, D. J., Yan, L., & Chen, J. J. (2015). Associations of resting-state fMRI functional connectivity with flow-BOLD coupling and regional vasculature. *Brain Connectivity*, *5*, 137-146.
- Tak, S., Wang, D. J., Polimeni, J. R., Yan, L., & Chen, J. J. (2014). Dynamic and static contributions of the cerebrovasculature to the resting-state BOLD signal. *NeuroImage*, *84*, 672-680.

- Thomson, A. M., & Bannister, A. P. (2003). Interlaminar connections in the neocortex. *Cerebral Cortex*, *13*, 5–14.
- Tian, P., Teng, I. C., May, L. D., Kurz, R., Lu, K., Scadeng, M., ... Devor, A. (2010). Cortical depth-specific microvascular dilation underlies laminar differences in blood oxygenation level-dependent functional MRI signal. *Proceedings of the National Academy of Sciences of the United States of America*, *107*, 15246–15251.
- Wang, Y., Robinson, J., Deshpande, G. (2016) *Resting state functional connectivity is sensitive to layer-specific connective architecture in cortical columns*. International Society for Magnetic Resonance in Medicine, Singapore. . p 636.
- Wang, Z., Chen, L. M., Negyessy, L., Friedman, R. M., Mishra, A., Gore, J. C., & Roe, A. W. (2013). The relationship of anatomical and functional connectivity to resting-state connectivity in primate somatosensory cortex. *Neuron*, *78*, 1116–1126.
- Wilson, G. H., III, Yang, P. F., Gore, J. C., & Chen, L. M. (2016). Correlated inter-regional variations in low frequency local field potentials and resting state BOLD signals within S1 cortex of monkeys. *Human Brain Mapping*, *37*, 2755–2766.
- Wu, R., Yang, P. F., & Chen, L. M. (2017). Correlated disruption of resting-state fMRI, LFP, and spike connectivity between area 3b and S2 following spinal cord injury in monkeys. *The Journal of Neuroscience*, *37*, 11192–11203.
- Wu, T. L., Mishra, A., Wang, F., Yang, P. F., Gore, J. C., & Chen, L. M. (2016). Effects of isoflurane anesthesia on resting-state fMRI signals and functional connectivity within primary somatosensory cortex of monkeys. *Brain and Behavior: A Cognitive Neuroscience Perspective*, *6*, e00591.
- Yacoub, E., Harel, N., & Ugurbil, K. (2008). High-field fMRI unveils orientation columns in humans. *Proceedings of the National Academy of Sciences of the United States of America*, *105*, 10607–10612.
- Zhao, F., Wang, P., Hendrich, K., Ugurbil, K., & Kim, S. G. (2006). Cortical layer-dependent BOLD and CBV responses measured by spin-echo and gradient-echo fMRI: Insights into hemodynamic regulation. *NeuroImage*, *30*, 1149–1160.

How to cite this article: Mishra A, Majumdar S, Wang F, Wilson III GH, Gore JC, Chen LM. Functional connectivity with cortical depth assessed by resting state fMRI of subregions of S1 in squirrel monkeys. *Hum Brain Mapp*. 2019;40:329–339. <https://doi.org/10.1002/hbm.24375>